INFLUENCE OF MICROSTRUCTURE ON THE FATIGUE PERFORMANCE OF PM STEELS

Ola Bergman and Anders Bergmark

Höganäs AB, SE-263 83 Höganäs, Sweden

ABSTRACT

The fatigue properties of PM steels are mainly depending on the microstructure and density. Focus of this article is to quantify the mechanical performance of PM steel materials based on mixed, pre-alloyed and diffusion-alloyed powders in relation to the microstructures. Fatigue performance is the target parameter and this has decided the amounts of graphite added to the base powders. With one exception, test samples were sintered for 30 minutes at 2050°F/1120°C in 90%N_2/10%H_2. Fatigue tests have been made in displacement controlled four-point plane bending on modified ISO 3928 specimens. No machining of the test bars was made. All materials have been tested at densities close to 7.1 g/cm^3. The PM steel microstructures are classified according to their fatigue performance. Sinter-hardened Astaloy CrM + 0.35%C with its martensitic microstructure has the highest fatigue limit of the tested materials (54 ksi/370 MPa). The diffusion-alloyed materials exhibit somewhat lower bending fatigue limits with D.HP + 0.8%C (48 ksi/330 MPa) followed by D.AE + 0.8%C (40 ksi/280 MPa). These materials demonstrate pronounced heterogeneous microstructures characterized by a continuous network of martensite with islands of softer structures. The pre-alloyed Astaloy CrL + 0.8%C with its mainly lower bainitic microstructure reaches a fatigue limit of 38 ksi/260 MPa. Astaloy Mo + 0.8%C has a microstructure dominated by upper bainite and reaches a fatigue limit of 31 ksi/210 MPa. The FC-0208 has a fatigue limit of 32 ksi/220 MPa and the microstructure consists mainly of fine pearlite.

INTRODUCTION

High fatigue performance of PM steels is an important parameter to introduce PM in new applications. One way to obtain high fatigue performance is to increase the density of the PM parts [1]. Also the microstructure is important for high performance PM steels. An optimized process for a specific application is a combination of density and choice of microstructure.

Several investigations on fatigue performance in relation to alloying system and processing are presented in the literature. Data has been reported by Sonsino [2], [3], [4]. Detailed studies of molybdenum pre-alloyed PM steels have been performed by Weiss et.al. [5]. A very comprehensive study was presented by Sanderow et. al. [6] in 1997. The study includes almost all PM steel alternatives used and they were investigated in as sintered as well as in heat-treated conditions. Investigations have also been presented by among others Lin et.al. [7], O'Brien [8], Bergmark [9], Cimino et.al. [10] and Engström et.al. [11].

A certain variation between different investigations is always found. Different experimental methods have been used. Alignment problems are also frequent in fatigue testing and this might influence some of the results. The main limitation, however, is that detailed information on the distribution and content of the microstructures are normally not included in the reports. Results from quenched PM steels reveal a rotating bending fatigue performance at density 7.1 g/cm^3 of about 380 MPa [6]. A scatter band of ±3 ksi/±20 MPa can also be estimated from the same investigation. Martensite is a beneficial microstructure from the fatigue performance point of view and it seems that the processing route to obtain martensite is not important. The other extreme considering performance is ferrite. Ferrite on the other hand or microstructures dominated by ferrite have normally low fatigue performance. No microstructure dominated by ferrite has been included in the study presented here. The mechanical performance of ferrite is well documented in the literature. Typically, ferritic PM steels at density 7.1 g/cm^3 has an axial fatigue limit of 100 MPa corresponding to a bending fatigue limit of about 120 MPa [6], [12]. Ferritic PM steels are never an alternative for high mechanical performance components.

In the present investigation six different PM steels sintered at 2050°F/1120°C for 30 minutes in 90%N_2/10%H_2 are studied. FC-0208 is a well-known material and it is included here as reference. Furthermore, one Mo pre-alloyed, one Cr-Mo pre-alloyed and three diffusion-alloyed materials are included in the study. Another Cr-Mo pre-alloyed material is high temperature sintered and sinter-hardened for comparison. The materials are characterized by microstructure and mechanical performance. The results allow a comparison between Mo and Cr-Mo materials. Important characteristics of diffusion-alloyed alternatives with more or less complex microstructures are pointed out. The design of the investigation allows conclusions both considering addition of single alloying elements and modifications of the microstructure as such. Detailed information on crack walk in relation to the microstructures can be found in a paper presented in Orlando 2002 [12].

EXPERIMENTAL PROCEDURE

Chemical compositions of the materials included in this study are presented in Table 1. Material A, FC-0208, is based on water-atomized ASC100.29 iron powder mixed with Cu (-150µm). Material B is pre-alloyed with 1.5%Mo. Material C is pre-alloyed with 1.5%Cr and 0.2%Mo, while material D is pre-alloyed with 3%Cr and 0.5%Mo. Material E is based on plain atomized iron powder diffusion-alloyed with 4%Ni, 1.5%Cu and 0.5%Mo. Materials F and G are based on a powder pre-alloyed with 1.5%Mo. Material F is diffusion-alloyed with 2%Ni, while material G is diffusion-alloyed with 4%Ni and 2%Cu. Carbon was admixed to all materials in the form of graphite (Kropfmühl UF4). The carbon contents given in Table 1 are desired as-sintered values. 0.8% Amide wax was used as lubricant.

Table 1. Chemical compositions of the investigated materials

Powder Mix		Fe (Wt.%)	Cr (Wt.%)	Cu (Wt.%)	Mo (Wt.%)	Ni (Wt.%)
A	FC-0208	Bal.	-	2	-	-
B	Astaloy Mo + 0.8%C	Bal.	-	-	1.5	-
C	Astaloy CrL + 0.8%C	Bal.	1.5	-	0.2	-
D	Astaloy CrM + 0.35%C	Bal.	3	-	0.5	-
E	D.AE + 0.8%C	Bal.	-	1.5	0.5	4
F	D.DC + 0.8%C	Bal.	-	-	1.5	2
G	D.HP + 0.8%C	Bal.	-	2	1.5	4

Modified ISO 3928 fatigue test bars with chamfered edges [12] and ISO 2740 standard tensile test bars were compacted to green density 7.1 g/cm^3. The test bars were sintered at 2050°F/1120°C for 30 minutes in 90%N_2/10%H_2. A normal cooling rate of 1.4°F/s / 0.8°C/s was applied. High temperature sintering at 2280°F/1250°C and sinter-hardening with a cooling rate of 5.4°F/s / 3°C/s was performed on material D. The sinter-hardened specimens were annealed at 360°F/180°C for 60 minutes in air.

Fatigue tests were carried out in displacement controlled 4 point plane bending mode at a frequency of 28 Hz and with load ratio R= $\sigma_{min}/\sigma_{max}$ = -1. The fatigue limit σ_A (50% estimated survival value) was determined by the stair case method with a run out limit of 2 million cycles and evaluated in accordance with MPIF standard No. 56, 2001. The staircase step (difference between adjacent stress levels) is chosen in the interval 4 – 5% of the estimated fatigue limit. Elongation and HV10 hardness were measured on the tensile specimens. Metallographic microstructures of the sintered samples were examined in light-optical microscope (LOM).

RESULTS

Sintered properties

Elongation and hardness values of the sintered test materials are presented in Table 2. Values for sintered density (SD) and carbon content are also included in the table. The measured carbon contents are in good agreement with what was aimed for (0.35% for material D and 0.8% for the other materials). All materials have a sintered density near 7.1 g/cm^3.

Table 2. Sintered Properties

Material	C (Wt.%)	SD (g·cm^{-3})	Elong. (%)	HV10
A	0.77	7.11	2.0	204
B	0.82	7.10	1.3	200
C	0.78	7.10	1.4	267
D*	0.33	7.14	1.5	377
E	0.82	7.12	1.6	252
F	0.83	7.11	0.9	246
G	0.85	7.13	1.1	285

*) High temperature sintered, sinter-hardened and annealed.

Elongation varies between 0.9% and 2.0% for the investigated materials. Hardness for the materials sintered at 2050°F (1120°C) is in the range of 200-285 HV10 whereas the high temperature sintered and sinter-hardened material has a hardness of 377 HV10.

Fatigue performance

Plane bending 50% estimated survival fatigue limits ($\sigma_{A,50\%}$) are presented in Table 3 and Figure 1.

The scatter obtained from the staircase method fatigue tests was generally small. Standard deviations below 0.7 ksi/5 MPa were found for most of the investigated materials. Materials C and D have higher standard deviations of 2.9 ksi/20 MPa and 5.1 ksi/35 MPa respectively.

Table 3. Plane Bending Fatigue Limits

Material	A	B	C	D*	E	F	G
$\sigma_{A,50\%}$ (ksi/MPa)	32.0/221	30.7/212	37.7/261	53.9/372	40.2/277	34.8/240	47.8/330

*) High temperature sintered, sinter-hardened and annealed.

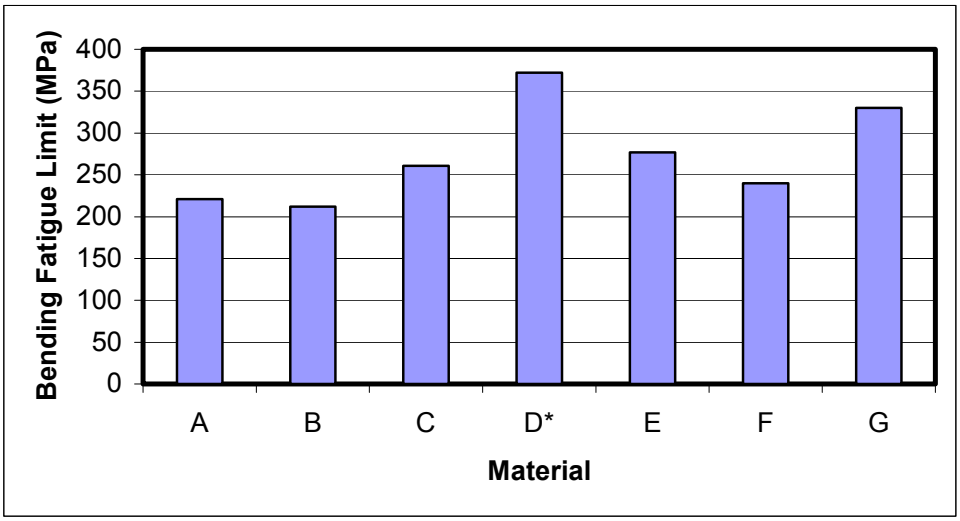


Figure 1. Plane bending 50% estimated survival fatigue limits at sintered density 7.1 g/cm^3.

The S-N diagram of FC-0208 (A) is shown in Figure 2. The low scatter evaluated from the staircase method is well illustrated in this diagram. The S-N diagram of Astaloy Mo + 0.8%C (B) (not shown here) reveals the same features.

Astaloy CrL + 0.8%C (C) has about 20% higher fatigue strength than FC-0208 and Astaloy Mo + 0.8%C (B). The S-N diagram of material C is shown in Figure 3. Some scatter in the data points can be observed for this material, which can be explained by metallographic observations (see next section).

The high fatigue endurance limit of martensite is demonstrated by sinter-hardened Astaloy CrM + 0.35%C (D). The material is high temperature sintered, sinter-hardened and tempered. The bending fatigue limit is 53.9 ksi/372 MPa. A relatively flatter S-N curve (not shown here) is found.

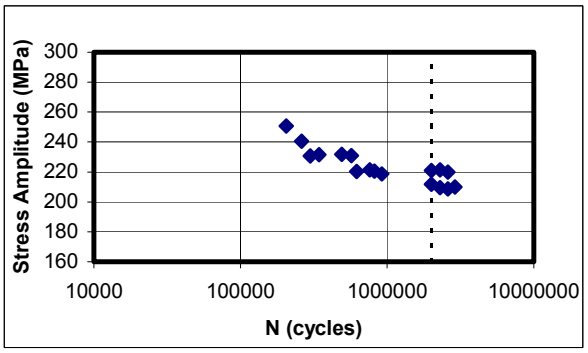


Figure 2. S-N diagram for FC-0208 in plane bending at sintered density 7.1 g/cm^3.

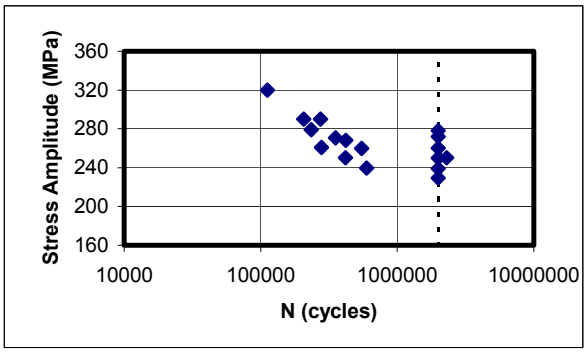


Figure 3. S-N diagram for Astaloy CrL + 0.8%C in plane bending at sintered density 7.1 g/cm^3.

The S-N diagram of the diffusion alloyed D.AE + 0.8%C (E) is shown in Figure 4. The fatigue limit of 40.2 ksi/277 MPa obtained from the staircase method is slightly higher than the fatigue limit for Astaloy CrL + 0.8%C (see Table 3). D.DC + 0.8%C (F) has a similar S-N curve (not shown here) as D.AE + 0.8%C (E).

D.HP + 0.8%C (G) has the best high-cycle fatigue properties of the materials sintered at conventional conditions, with the bending fatigue limit 47.8 ksi/330 MPa. The S-N diagram of D.HP + 0.8%C is shown in Figure 5. The ”knee-point” of the S-N curve is obtained at less than 100.000 cycles.

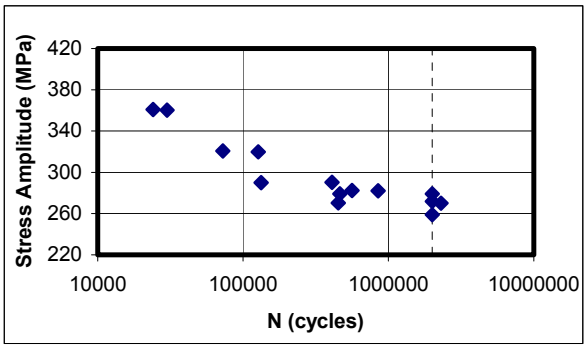


Figure 4. S-N diagram for D.AE + 0.8%C in plane bending at sintered density 7.1 g/cm^3.

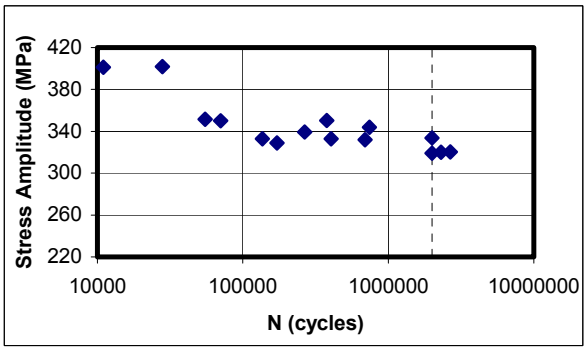


Figure 5. S-N diagram for D.HP + 0.8%C in plane bending at sintered density 7.1 g/cm^3.

Microstructures

The microstructure of FC-0208 is almost fully pearlitic (see Figure 6). Most of the microstructure consists of fine pearlite, where the cementite lamellas are thin and closely packed together. Some areas of coarse pearlite and ferrite are also present. Astaloy Mo + 0.8%C (B) has a microstructure that consists of mainly upper bainite characterized by carbides irregularly distributed between ferrite regions (see Figure 7). Small areas of lower bainite are also observed with fine carbides that are distributed between as well as within the ferrite regions.

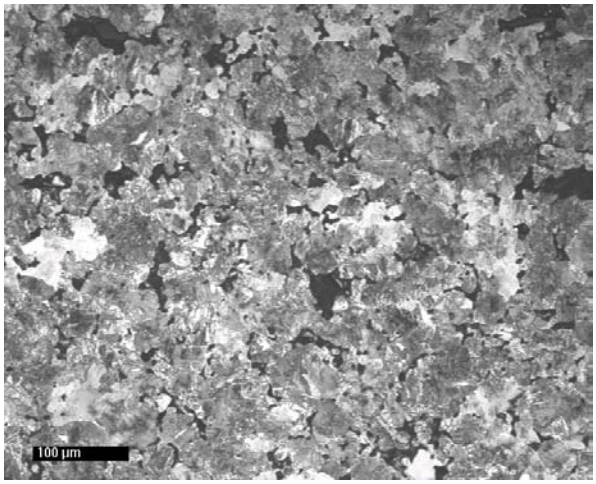


Figure 6. Microstructure of FC-0208 (0.77%C). Etched with Picral.

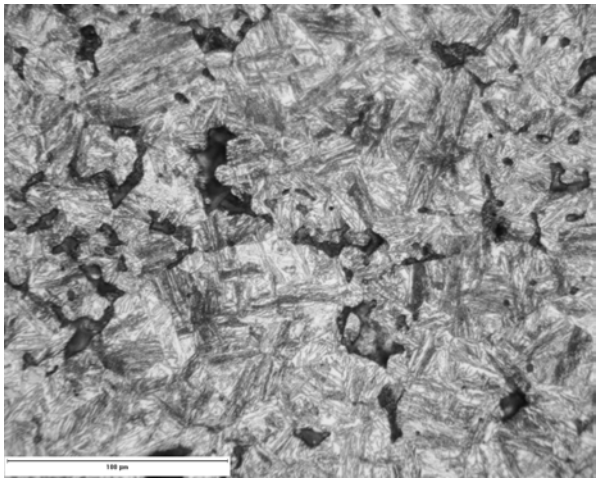


Figure 7. Microstructure of Astaloy Mo + 0.82%C. Etched with Nital.

The microstructure of Astaloy CrL + 0.8%C is presented in Figure 8. Lower bainite dominates with some regions of upper bainite and martensite. The microstructure of sinter-hardened and tempered Astaloy CrM + 0.35%C with a mixture of martensite and lower bainite is shown in Figure 9. Small areas of upper bainite can also be observed. The relatively low carbon content in the material explains why the microstructure is not fully martensitic although rapid cooling was applied. Some variation of the relative content of the metallographic phases was found between individual samples. This is probably due to that the samples have experienced somewhat different cooling rates during processing and it is the reason for the scatter in fatigue performance obtained for these two materials.

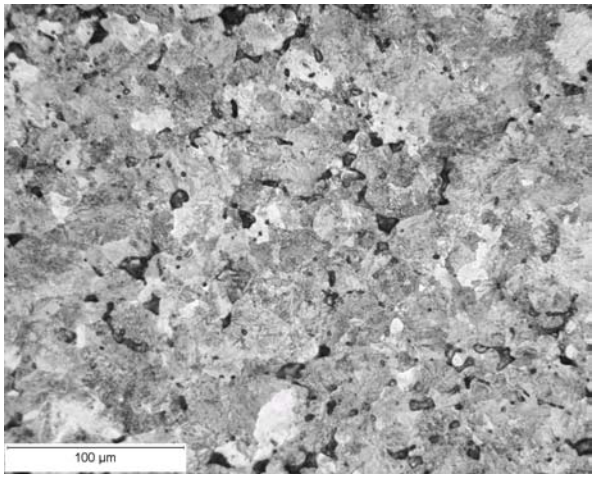


Figure 8. Microstructure of Astaloy CrL + 0.78%C. Etched with Nital/Picral.

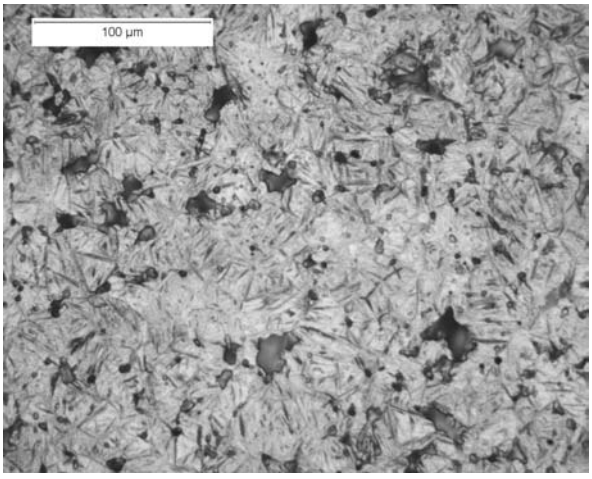


Figure 9. Microstructure of Astaloy CrM + 0.33%C. Etched with Nital/Picral.

D.AE + 0.8%C has a microstructure that consists of pearlite mixed with martensite and austenite (see Figure 10). The heterogeneous microstructure is a consequence of the relatively low diffusion rate of Mo and Ni in solid state at the sintering temperature 2050°F/1120°C. Martensite is formed in Cu-rich areas in combination with Mo. Martensite is also formed as a shell around Ni-rich austenitic areas. The core of the base particles contains mainly pearlite.

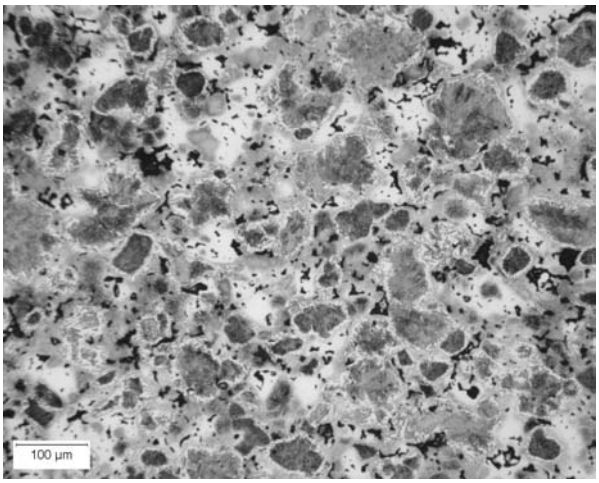


Figure 10. Microstructure of D.AE + 0.82%C. Etched with Picral.

The microstructure of D.DC + 0.8%C is dominated by upper bainite (see Figure 11). The upper bainite areas originate from the base powder particles pre-alloyed with 1.5%Mo (compare with Figure 7). A network of martensite surrounding areas of Ni-rich austenite is also seen.

The microstructure of D.HP + 0.8%C, which is presented in Figure 12, is also heterogeneous with a combination of the features characterizing D.AE + 0.8%C and D.DC + 0.8%C. The microstructure contains martensite, lower bainite, upper bainite and austenite. The martensitic network in D.HP + 0.8%C is much more pronounced and the bainitic areas smaller. The network is formed by Cu-rich martensite mainly surrounding the pores and Ni-rich martensite surrounding Ni-rich austenite.

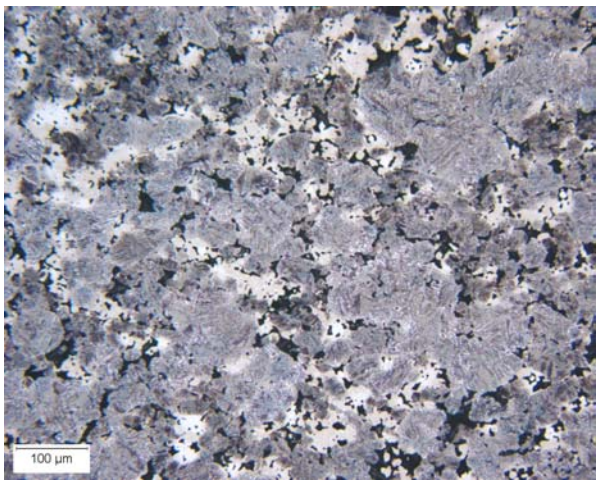


Figure 11. Microstructure of D.DC + 0.83%C. Etched with Picral.

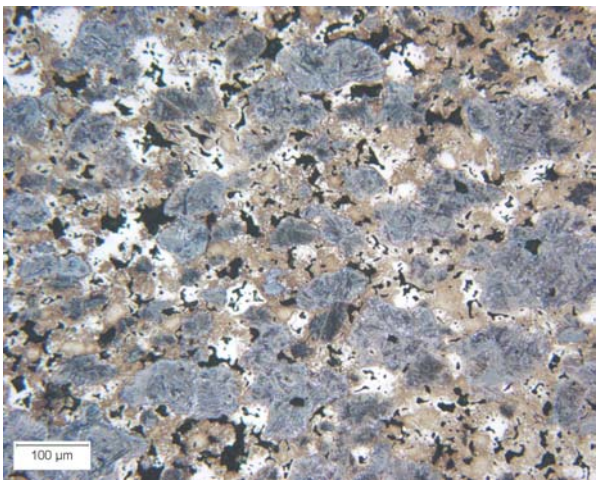


Figure 12. Microstructure of D.HP + 0.85%C. Etched with Picral.

DISCUSSION

This study was made on the mechanical performance of different PM steels. Focus is on plane bending fatigue performance and the results allow a classification of the materials based on the microstructures.

Martensitic microstructures are beneficial for the fatigue performance of PM steels. Four materials in the present study contain martensite. The highest performance is found for sinter-hardened Astaloy CrM + 0.35%C. The microstructure reveals a mixture of martensite and bainite. However, martensite dominates and the fatigue limit found is similar to data (52-58 ksi/360-400 MPa) presented in the literature for fully martensitic materials [6].

The importance of distribution of the metallographic phases in heterogeneous diffusion-alloyed PM steels is well illustrated by the three diffusion-alloyed materials included in the study. D.DC + 0.8%C contains a soft matrix (low yield stress) of upper bainite with islands of Ni-rich austenite surrounded by a strong shell of martensite. The microstructure of Astaloy Mo + 0.8%C is dominated by upper bainite. The 13% higher fatigue limit of D.DC + 0.8%C is due to the presence of the Ni-rich islands. D.AE + 0.8%C and D.HP + 0.8%C on the other hand have the reversed relation between strong and soft phases. A strong matrix is formed with Cu-rich martensite and Ni-rich islands surrounded by martensite. Relatively softer isolated islands of pearlite in D.AE + 0.8%C and upper bainite in D.HP + 0.8%C are found in the strong martensitic network.

Finally, a comment on the scatter obtained from the staircase method fatigue tests. Generally, the scatter obtained is very small. The step (difference between adjacent stress levels) used is 4 – 5% of the expected fatigue endurance limit. The calculated standard deviation is often below half of the step. Typically, standard deviations below 5 MPa are found. This indicates that the crack initiation mechanisms are well defined and also well represented in the material. This is an index of high reliability of the mechanical performance found.

CONCLUSIONS

- The microstructure composition has strong influence on the fatigue performance of PM steels.
- High temperature sintered and sinter-hardened Astaloy CrM + 0.35%C with mainly martensitic microstructure has a very high bending fatigue limit of 54 ksi/370 MPa.
- Fine pearlite in FC-0208 and upper bainite in Astaloy Mo + 0.8%C have similar bending fatigue limits (31-32 ksi/210-220 MPa), while the fatigue limit for lower bainite in Astaloy CrL + 0.8%C is about 20% higher (38 ksi/260 MPa).
- A well-controlled distribution of metallographic phases in heterogeneous microstructures gives high fatigue strength. Microstructures characterized by a martensitic network with islands of upper bainite in D.HP + 0.8%C give a high fatigue limit of 48 ksi/330 MPa. For D.AE + 0.8%C, where islands of pearlite are surrounded by a martensitic network, the fatigue limit is 40 ksi/280 MPa.
- The scatter of the fatigue strength evaluated from the staircase method in this investigation is generally small.

REFERENCES

1. Bergmark, A. “Influence of Density on PM Steel Fatigue Crack Initiation and Propagation”, *Metal Powder Industries Federation, Advances in Powder Metallurgy and Particulate Materials*, New Orleans, 2001.
2. Sonsino, C.M. “Ermittlung anwendungsrelevanter Kenngrössen für Sintermetalle”, LBF FhG. Bericht Nr. FB-158, 1981 (in German)
3. Sonsino, C.M. “Schwingfestigkeit von Verschidenen Sinterstahählen und bemessungskriterien für Gesinterte Bauteile”, LBF-FhG. Bericht Nr. FB 170,1984 (in German).
4. Sonsino, C.M. “Einfluss Sintertechnischer Grensen für die Herstellung von Schwingbeanspruchten Bauteilen aus Sinterstahl”, LBF FhG. Bericht Nr. FB-184,1989 (in German).
5. Weiss, B., Danninger, H. and Hadrboletz, A. “Review of the Fatigue Behavior of Pressed and Sintered Ferrous Materials”, European Powder Metallurgy Association, Proceedings of the 1998 Powder Metallurgy World Congress, Granada 1998.
6. Sanderow, H.I., Spirko, J.R. and Friedhoff, T.G. “Fatigue properties of P/M materials: Relationship to RBF and AF results to Material-Processing Parameters”, *Metal Powder Industries Federation, Advances in Powder Metallurgy and Particulate Materials*, Vol. 2, pp. 117-135, 1997.
7. Lin, S-Y, Prucher, T. and Friedhoff, T.G. “A Comparison of Tensile, Rotating Bending Fatigue and Axial Fatigue Test Results of P/M Alloys”, *Metal Powder Industries Federation, Advances in Powder Metallurgy and Particulate Materials*, Vol. 7, pp. 381-389, 1994.
8. O’Brien, R.C. “Fatigue Properties of P/M Materials”, SAE Congress, Michigan, Febr-March, 1988
9. Bergmark, A. ”Materialdata för PM stål med varierade ytor och geometrier”, Jernkontorets forskning Serie D, 763, Jernkontoret, Stockholm Sweden 1999 (in Swedish).

10. Cimino, T.M., Graham, A.H., Murphy, T.F. “Effect of Microstructure and Pore Morphology on Mechanical and Dynamic Properties of Ferrous P/M Materials”, *Industrial Heating*, Vol. 67, no. 9, pp. 93-96, 2000.
11. Engström, U., Lipp, K., Sonsino, C.M.” Influence of notches on fatigue strength of high performance PM materials”. *Metal Powder Industries Federation, Advances in Powder Metallurgy & Particulate Materials* - 2001 (USA), pp. 9, 2001
12. Bergmark, A., Alzati, L., Persson, U. ”Fatigue Crack Initiation in PM Steels”, *Metal Powder Industries Federation, Advances in Powder Metallurgy and Particulate Materials*, Orlando, 2002.